MODELING OF SUPERSONIC REACTING FLOW FIELDS

J. P. Drummond and H. S. Mukunda
NASA Langley Research Center
Hampton, Virginia 23665

Work has been underway for a number of years, both in the United States and abroad, to develop advanced aerospace propulsion systems for use late in the century and beyond. One such program is now underway at the NASA Langley Research Center to develop a hydrogen-fueled supersonic combustion ramjet, also known as a scramjet, that is capable of propelling a vehicle at hypersonic speeds in the atmosphere or beyond the atmosphere into orbit. A part of that research has recently been directed toward the optimization of the scramjet combustor, and in particular the efficiency of fuel-air mixing and reaction taking place in the engine. In the very high speed vehicle configurations currently being considered, achieving a high combustor efficiency becomes particularly difficult. This is a consequence of the fact that with increasing vehicle Mach number, the average Mach number in the combustor also increases. As the combustor Mach number increases, the degree of fuel-air mixing that can be achieved through natural convective and diffusive processes is reduced, leading to an overall decrease in combustion efficiency and thrust.

From the above discussion, it is clear that a detailed understanding of the scramjet combustor flow field is critical to the achievement of a successful design. Even though the combustor flow field is quite complex, it can be realistically viewed as a collection of spatially developing and reacting supersonic mixing layers that are initially discrete, but that ultimately merge into larger more complex zones. These mixing layers begin downstream of a set of fuel injectors that introduce gaseous hydrogen in both a parallel and transverse direction into a supersonic air stream entering from the engine inlet. The behavior of the initial portion of the combustor flow, in the mixing layers near the fuel injectors, appears to be most critical, since this is where the mechanism for efficient high speed mixing must be established to achieve the required degree of combustion downstream. Because of the structure of the flow field in this initial portion of the combustor, a single supersonic, spatially developing and reacting mixing layer serves as an excellent physical model for the overall flow field. Even though this reacting mixing layer flow is geometrically simple, it can still be made to retain all of the fluid mechanical and chemical complexitites present in the actual combustor flow field.

Prior studies on supersonic reacting mixing layers have been quite limited. A fair amount of work has been carried out, however, on nonreacting mixing layers both at subsonic and supersonic speeds. Even without combustion, the results of these studies provided a significant amount of useful information for understanding reacting layers. A review of nonreacting mixing layer studies was given in references 1, 2, and 3, and the

reader is referred to those papers for further discussion. Many of the important features described for nonreacting layers also occurred in reacting layers. The subsonic and supersonic reacting literature is also reviewed in references 1, 2, and 3.

Because of the difficulties described earlier for achieving a high supersonic combustion efficiency, attention has now turned to the development of techniques for enhancing the rate of fuel-air mixing in the combustor. The supersonic mixing layer is again providing an excellent physical model for carrying out these studies. Several efforts in this area are discussed in reference 4. One effort, now underway at the NASA Langley Research Center, involves a numerical study of fuel-air mixing in a two-dimensional or three-dimensional supersonic, spatially developing and reacting mixing layer. Two-dimensional studies are reported here; three-dimensional studies are now underway. In this work, several techniques have been applied to enhance the mixing processes and overall combustion efficiency in the mixing layer. Based on the results of this study, an alternate fuel injector configuration was designed computationally, and that design increased the amount of fuel-air mixing that was achieved. Details of this work are reported in reference 4. The results in that paper are summarized in the following discussion and figures.

Once the theory and solution procedure described in reference 4 had been developed and coded, several spatially developing mixing layer flows were simulated using the computer program. The code was first checked by comparing with a known exact solution by Lock for a spatially developing mixing layer.[4] The comparison of Lock's solution with the code (SPARK) is shown in figure 1 where the nondimensional streamwise velocity is plotted against η, the similarity variable across the layer. The agreement between the code and theory is excellent. The program was then applied to reacting mixing layer cases to assess several candidate configurations for enhancing fuel-air mixing and reaction. The first of these cases, shown in figure 2, served as a benchmark calculation in that it contained no enhancement mechanism. Case 1 involved a mixing layer developing between a fuel stream and an air stream that were initially separated by a thin splitter plate. The fuel stream was made up a mixture of ten percent hydrogen and ninety percent nitrogen introduced above the plate at a velocity of 2672 m/s, a temperature of 2000K, and a pressure 0.101 MPa (1 atm.) Air was introduced below the plate at a velocity of 1729 m/s, a temperature of 2000K and a pressure of 0.101 MPa. These conditions resulted in a Mach number of 2 for both streams. Contours of streamwise velocity, temperature and water mass fraction are given in figure 3. These results over a length of 10 cm. show a slow laminar spread of the layer with little mixing until well downstream, where a Kelven-Helmholtz instability occurs. Enchancement is clearly required.

In an attempt to enhance the mixing, the mixing layer under the same conditions, was then processed through two 10° planar shocks using the configuration shown in figure 4 (Case 2). Resulting contours of velocity, temperature, and water mass fraction are again shown in figure 5. There is some enhancement of mixing and reaction, but a

higher degree of mixing is required. The final attempt to enhance the benchmark case is described in figure 6. A small body is placed in the mixing layer, resulting in the formation of a curved bow shock. When the high velocity gradient of the mixing layer is processed by the curved shock, vorticity is produced. This results in significantly enhanced mixing as can be seen from the contours in figure 7. Large scale structure is produced, and there is appreciable growth of the layer in this case. A quantitative comparison of cases 1 through 3 is given in figures 8 and 9 which show mixing and combustion efficiency plotted versus streamwise distance. Case 3 is clearly superior to cases 1 and 2.

Based on these results, a simple modification to a conventional scramjet strut shown in figure 10 was considered. Gaseous hydrogen fuel is typically injected from the base of the struts, parallel to the inlet air into the combustor, and perpendicular to the inlet air from a location behind a rearward facing step. In the "modified" strut design, the parallel fuel injector was moved from the strut base to the rearward facing step. From there, the parallel jet was processed by a curved low shock lying ahead of the transverse jet, resulting in a situation similar to case 3. When the high velocity gradient of the parallel jet interacted with the bow shock, vorticity was produced, and mixing was enhanced downstream.

For comparison, the modified strut with only the parallel jet injecting hydrogen was considred in case 4. The resulting velocity, temperature, and water mass fraction contours (using an 18 step H_2-air finite rate model) for this case are shown in figure 11. Significant mixing is delayed until well downstream along the jet axis. When an identical amount of gaseous hydrogen is injected from the transverse jet in case 5, however, a significant degree of mixing occurs well upstream. The enhanced mixing can clearly be seen in the velocity, temperature, and water contours in figure 12 along with a much higher degree of structure. A quantitative comparison of cases 4 and 5 is given in the mixing and combustion efficiency plots of figures 14 and 15, respectively. Even though twice the hydrogen is being injected in case 5 as compared to case 4, only half the streamwise distance is required in the enhanced case 5 to achieve the same level of mixing and combustion efficiency ultimately reached in the unenhanced case 4. The modified strut configuration therefore significantly increased the amount of fuel-air mixing and reaction that was achieved over a given combustion length.

REFERENCES

1. Drummond, J. P.; Rogers, R. C.; and Hussaini, M. Y.: A Numerical Model for Supersonic Reacting Mixing Layers. Computer Methods in Applied Mechanics and Engineering, V.64, pp. 39-60.

2. Drummond, J. P.; and Hussaini, M. Y.: Numerical Simulation of a Supersonic Reacting Mixing Layer. AIAA Paper No. 87-1325, June 1987.

3. Drummond, J. P.: Two Dimensional Numerical Simulation of a Supersonic Chemically Reacting Mixing Layer. NASA TM, 1988.

4. Drummond, J.P.; and Mukunda, H. S.: A Numerical Study of Mixing Enhancement in Supersonic Reacting Flow Fields. AIAA Paper No. 88-3260, July 1988.

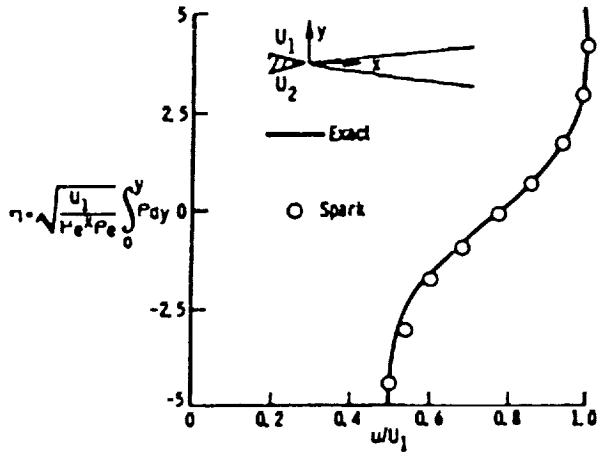

Fig.1 - Comparison of the computation with the exact solution of Lock.

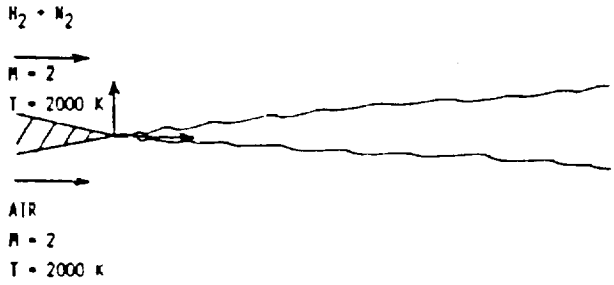

Fig 2 - Schematic of the supersonic reacting mixing layer in Case 1.

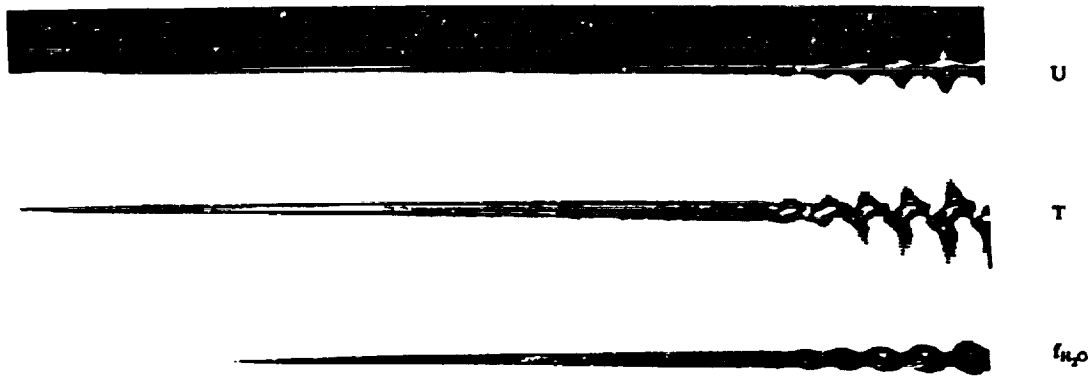

Fig.3 - Velocity, temperature, and water mass fraction contours in Case 1.

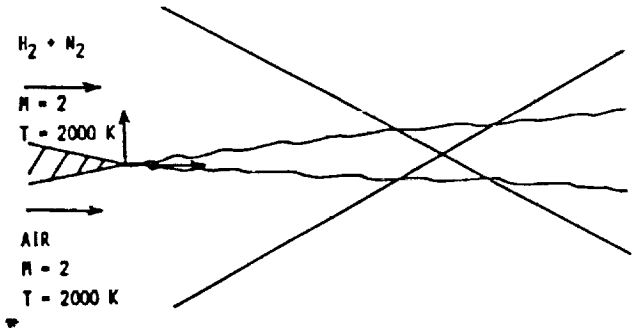

Fig.4 - Schematic of the supersonic reacting mixing layer interacting with two shocks in Case 2.

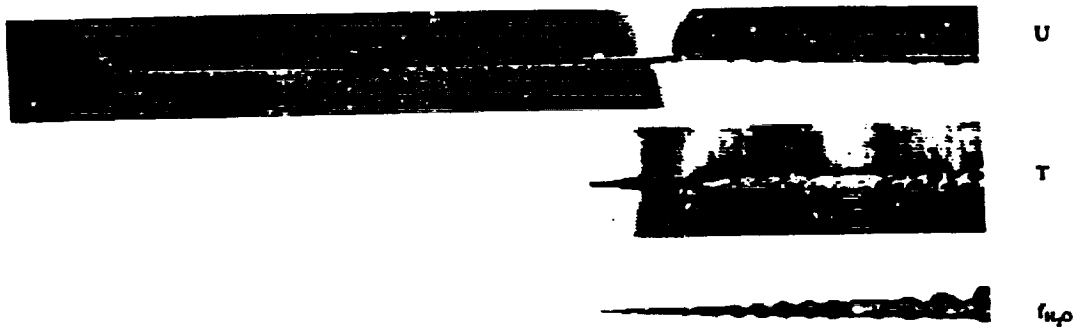

Fig.5 - Velocity, temperature, and water mass fraction contours in Case 2.

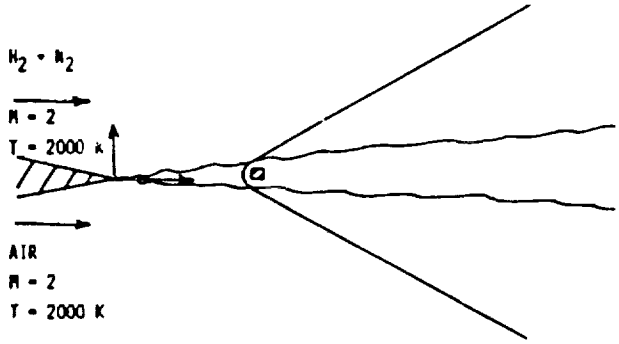

Fig.6 - Schematic of the supersonic reacting mixing layer interacting with a curved shock in Case 3.

Fig.7 - Velocity, temperature, and water mass fraction contours in Case 3.

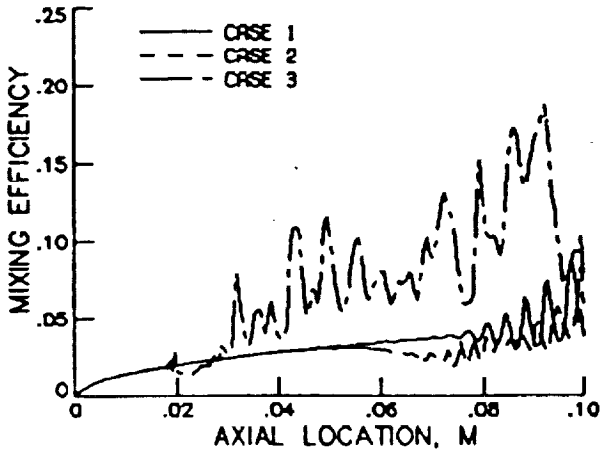

Fig.8 - Mixing efficiency versus streamwise station for Cases 1 through 3.

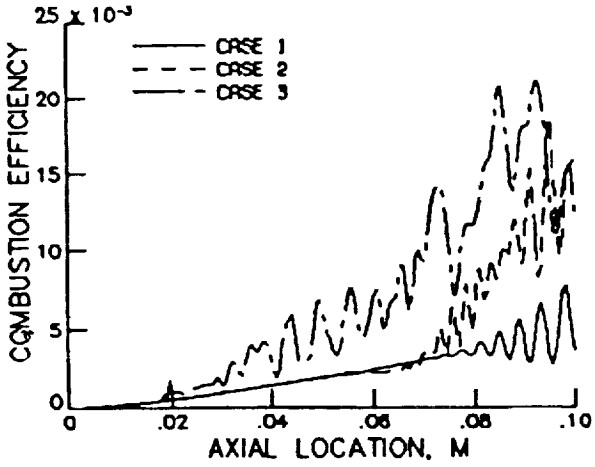

Fig.9 - Combustion efficiency versus streamwise station for Cases 1, 2 and 3.

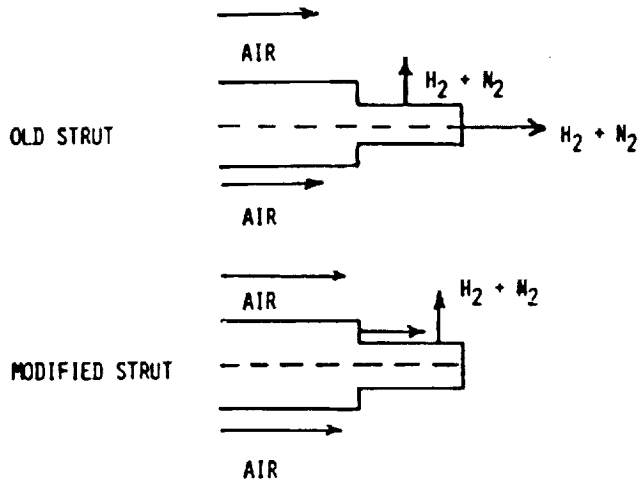

Fig.10 - Schematic of conventional and modified fuel injector strut configurations.

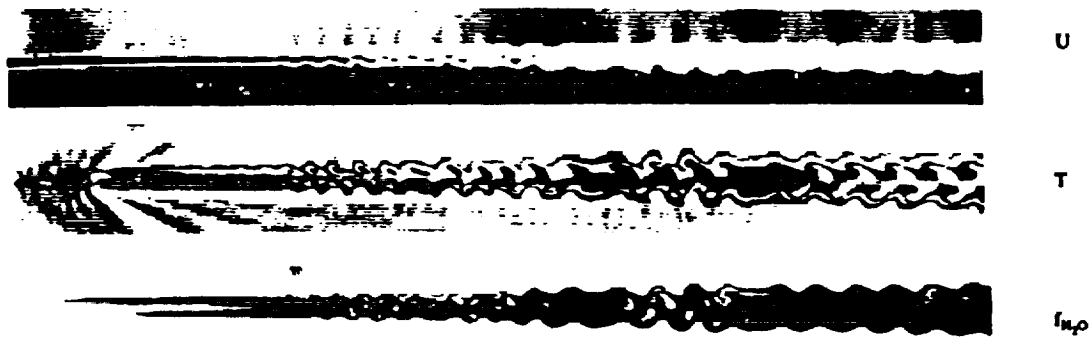

Fig.11 - Velocity, temperature, and water mass fraction contours in Case 4 with only the parallel injector.

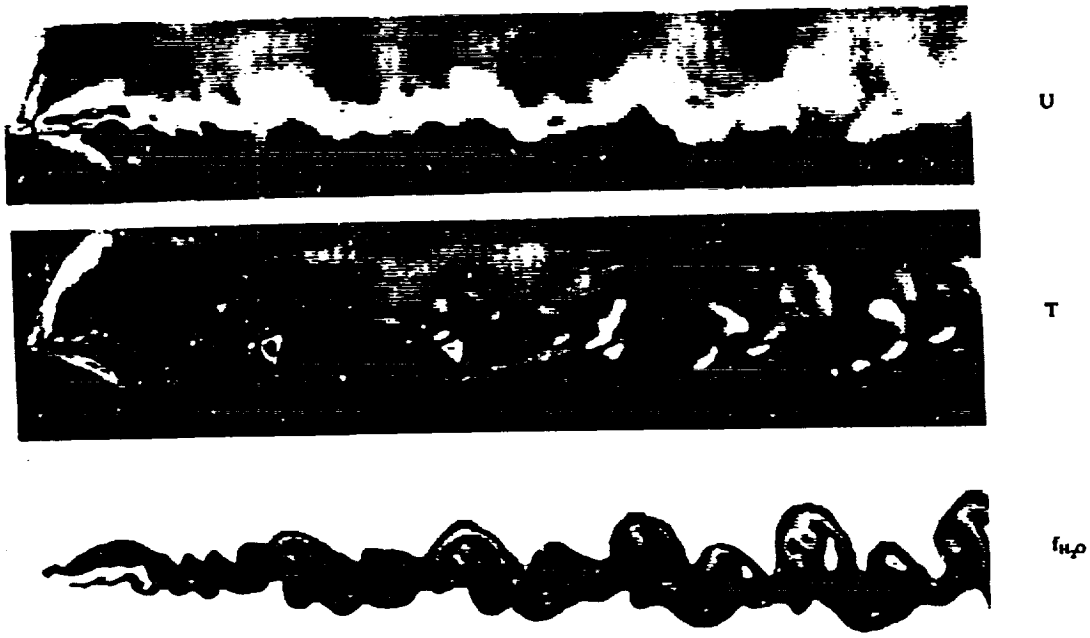

Fig.12 - Velocity, temperature, and water mass fraction contours in Case 5 with interaction of the parallel and transverse injectors.

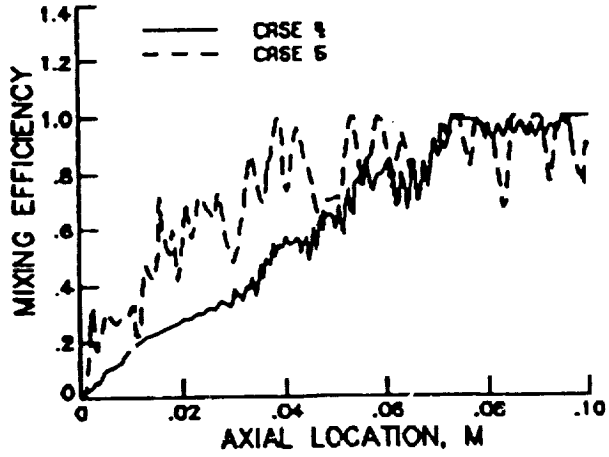

Fig.13 - Mixing efficiency versus streamwise station for Cases 4 and 5.

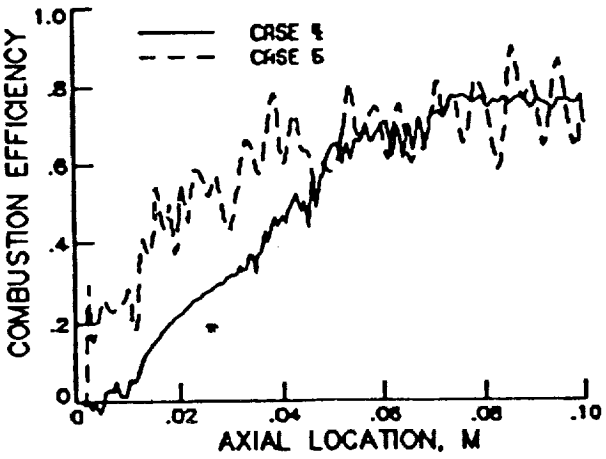

Fig.14 - Combustion efficiency versus streamwise station for Cases 4 and 5.